Physical Drivers of the November 2023 Heatwave in Rio de Janeiro

Catherine C. Ivanovich[1], Adam H. Sobel[1,2,3], Radley M. Horton[2,4], Ana M. B. Nunes[5], Rosmeri Porfírio da Rocha[6], and Suzana J. Camargo[2,4]

[1]Department of Earth and Environmental Sciences, Columbia University, New York, NY, United States
[2]Lamont-Doherty Earth Observatory, Columbia University, Palisades, NY, United States
[3]Department of Applied Physics and Applied Mathematics, Columbia University, New York, NY, United States
[4]Columbia Climate School, Columbia University, New York, NY, United States
[5]Instituto de Geociências, Universidade Federal do Rio de Janeiro, Rio de Janeiro, RJ, Brazil
[6]Instituto de Astronomia, Geofísica e Ciências Atmosféricas, Universidade de São Paulo, São Paulo, SP, Brazil

Correspondence to: Catherine Ivanovich (cci2107@columbia.edu)

15 **Abstract.** As extreme heat has not historically been a major hazard for the city of Rio de Janeiro,
16 the November 2023 Heatwave magnitude and timing were staggering. Here we conduct a case
17 study of reanalysis data and high-resolution projections to explore the event drivers and
18 characterize the evolving extreme heat risk in the city of Rio de Janeiro. We find that the
19 heatwave was associated with atmospheric blocking, potentially linked to the 2023-24 El Niño
20 event. Soil moisture declines increased surface sensible heat flux, and elevated sea surface
21 temperatures reduced coastal cooling. The heatwave was preceded by weeks of suppressed
22 precipitation and terminated by the onset of rain. We also find a significant historical increase in
23 the frequency of high heat days throughout Brazil and a lengthening of the heat season in the city
24 of Rio de Janeiro. The frequency of the city's austral spring heat extremes is expected to increase
25 further in the future, highly dependent upon our future emissions pathway. These results
26 emphasize the rapidly emerging risk for extreme heat in the city of Rio de Janeiro.

28 **1 Introduction**

29 In the spring of 2023, the city of Rio de Janeiro experienced a high impact heatwave that
30 caught the world's attention. Media sources ranging from local reporting to international news
31 companies centered stories on the event's record-breaking temperature magnitudes and
32 unseasonal timing, arriving earlier in the warm season than typical heatwaves (Correio
33 Braziliense, 2023; Hughs and Jeanet, 2023). The impacts of the extreme heat were widely
34 publicized in part due to the tragic death of a concertgoer hospitalized during a Taylor Swift
35 performance in Rio de Janeiro on November 17, with news articles reporting heat-induced
36 cardiovascular distress as the cause of death (Nguyen, 2023). Sources also report that the stadium
37 in which the concert took place experienced higher temperatures than those measured in the open
38 air, as well as a lack of cooling equipment and insufficient water for attendees (Nguyen, 2023;
39 Jornal Nacional, 2023). Such complexities highlight that extreme heat experienced by
40 individuals on the ground can far exceed temperatures measured at local weather stations,
41 depending on infrastructure and the capacity for cooling interventions (Wilby et al., 2021; Nahlik
42 et al., 2017). However, the meteorological event itself is of course one of the preconditions for
43 societal impacts. We therefore explore the physical mechanisms behind the heatwave as one key
44 step towards improving preparation for the impact of future extreme heat events.

45 Throughout Brazil, the highest temperatures occur climatologically in low latitude and

46 low altitude regions in the interior of the country, such as the cities of Teresina (Piauí, in the

47 Northeast region of Brazil) and Palmas (Tocantins, in the Central-West region of Brazil; Alvares

48 et al., 2013), both of which are far from Rio de Janeiro. Extreme temperatures tend to be

49 intensified by land-atmosphere interactions, as dry soils partition more energy into sensible heat

50 (Geirinhas et al., 2018). These relationships between the atmosphere and land surface processes

51 increase the likelihood of compound extreme heat and drought events and intensify impacts on

52 agriculture (Cirino et al., 2015), worker productivity for outdoor laborers (Bitencourt et al.,

53 2021), wildfire risk (Libonati et al., 2022), and direct impacts on human health (Zhao et al.,

54 2019). As the frequency and intensity of extreme heat throughout Brazil has increased

55 significantly in the past decades and is projected to continue in the future (Feron et al., 2019;

56 Regoto et al., 2021; Bitencourt et al., 2020), the widespread socio-economic impacts of these

57 events are likely to grow.

58 While Rio de Janeiro is the second most populous city in Brazil (Instituto Brasileiro de

59 Geografia e Estatística 2022) and the third most populous city in South America (United Nations

60 Department of Economic and Social Affairs Population Division 2022), few studies have

61 focused on extreme heat in the city. On one hand, Rio de Janeiro has not historically been a

62 major hotspot of extreme heat in Brazil and has experienced fewer heatwaves relative to other

63 major cities in the country (Geirinhas et al., 2018). Further, the numerous microclimates within

64 the city, influenced by its coastal setting and complex topography, complicate the study of local

65 heatwave dynamics. Indeed, there is large spatial variability in temperature extremes across the

66 Rio de Janeiro metropolitan area compared to other Brazilian cities (Alvares et al., 2013).

67 However, impactful heatwaves in recent decades have increasingly drawn attention from public

68 health officials and scientific communities alike. Recent literature has explored the dynamics and

69 mortality impacts of extreme temperatures during heatwaves in 2010 (Geirinhas et al., 2019) and

70 2013/2014 (Geirinhas et al., 2022) and has begun to investigate compound heatwave and drought

71 events throughout Southeast Brazil (Geirinhas et al., 2021). There is also building evidence that

72 temperature extremes are increasing in intensity and frequency throughout Brazil, including the

73 city of Rio de Janeiro (Regoto et al., 2021; Bitencourt et al., 2019). Climate variability also plays

74 an important role in modulating temperatures over this area, including large scale modes of

75 climate variability such as the El Niño-Southern Oscillation (Rehbein and Ambrizzi 2023; Cai et

78   al., 2020; Shimizu and Ambrizzi 2015), the Pacific Decadal Oscillation, and the Atlantic

79   Multidecadal Oscillation (He et al., 2021). Should more intense, frequent, and unseasonably

80   early extreme heat events take place in the future in the city of Rio de Janeiro, these heatwaves

81   may have increased impacts on human health due to potential exceedance of unprecedented

82   temperature thresholds and individuals' lack of preparation for these events. In a tropical city

83   where baseline temperatures are already relatively high, small shifts in the temperature

84   distribution can have large impacts on the frequency of extremes (Cheng et al., 2019),

85   particularly at thresholds relevant to human health outcomes (Vecellio et al., 2022). These health

86   risks are compounded by the humidity in Rio de Janeiro, a coastal city with ample moisture

87   sources from the ocean and surrounding vegetation, priming the region for humid heat extremes

88   which are physiologically more dangerous to human health than dry heat (Mora et al., 2017).

89   In this study, we explore the meteorological conditions that led to the extreme heat event

90   in November 2023 in the city of Rio de Janeiro. We identify drivers of the exceptional

91   magnitude and persistence of the extreme temperatures, as well as their early arrival in the

92   calendar year. We compare these conditions to those associated with typical heatwaves in the

93   region, and particularly events taking place in the spring season. We then consider how extreme

94   spring temperature events have shifted throughout the historical period, and how we might

95   expect them to change in the future with ongoing anthropogenic climate change.

96

97   **2 Methods**

98   **2.1 Data**

99   This analysis employs both station-based observations and reanalysis data. Initial

100   analyses are conducted on subdaily station data from the city of Rio de Janeiro, accessed via the

101   Met Office Hadley Center's HadISD station-based dataset (Dunn 2019) and the Rio Alert

102   System produced by the Rio de Janeiro City Hall (Sistema Alerta Rio da Prefeitura do Rio de

103   Janeiro 2024). Three airport weather stations are available from HadISD for the city of Rio de

104   Janeiro, namely the Galeão/Antonio Carlos Jobim International Airport (located on the island

105   Ilha do Governador within the Guanabara Bay), the Campo Délio Jardim De Mattos Airport (an

106   Air Force base located in the city's North Zone), and the Santos Dumont Airport (a waterfront

107   airport located near the city center). Six additional stations from the Rio Alert System dataset

108   record measurements from the tops of various community and commercial buildings, including

109   hotels, schools, and warehouses. These stations are located in distinct areas of the city, whose

110   topographical and coastal complexities contribute to various microclimates. These stations thus

111   record distinct values, both instantaneously and on average (see Fig. S1), a challenge that has

112   been previously identified in the literature (Lyra et al., 2018; Dereczynski et al., 2013). We

113   therefore base the majority of our analysis on reanalysis data and compare the identified patterns

114   with station data when possible. This comparison is particularly important for extreme events, as

115   the magnitude of extreme heat has been shown to be biased in reanalysis products due to their

116   spatial and temporal smoothing of observations (Rogers et al., 2021; Raymond et al., 2020).

117   Further, the human experience of heat stress is inherently hyperlocal, meaning that the distinct

118   microclimates existing throughout the city can control heat stress exposure and the efficiency of

119   adaptation strategies. However, the present study is primarily concerned with the regional drivers

120   of the extreme event rather than its absolute magnitude. Reanalysis provides continuous spatial

121   coverage and a wide array of internally consistent meteorological variables, which warrants its

122   use for the application here.

123   Hourly meteorological data are retrieved from the fifth major global reanalysis of the

124   European Centre for Medium-Range Weather Forecasts (ERA5), including 2-meter temperature,

125   2-meter dewpoint temperature, volumetric soil water for layer 1 (0-7 cm, where the surface is at

126   0 cm), surface pressure, geopotential height at 500 hPa and 200 hPa, precipitation, evaporation,

127   2-meter horizontal winds, and vertical velocity at 500 hPa (Hersbach et al., 2020). From this

128   hourly data, daily maximum temperature, daily total precipitation, and daily means of all other

129   variables are calculated from 1979-2023. Daily mean sea surface temperature (SST) data from

130   1979-2023 is also retrieved from the NOAA 1/4° Daily Optimum Interpolation Sea Surface

131   Temperature (OISST) dataset (Huang et al., 2021).

132   We also explore the future evolution of temperature extremes over the city of Rio de

133   Janeiro using the NEXGDDP dataset (Thrasher et al., 2022). This data product is statistically

134   downscaled from the Coupled Model Intercomparison Project Phase 6 (CMIP6) models, with a

135   spatial resolution of 0.25 degrees and outputs variables on a daily temporal scale. We directly

136   retrieve daily maximum temperature data through the end of the century under the Shared

137   Socioeconomic Pathways (SSPs) SSP2-4.5 and SSP5-8.5 for the 23 models which output this

138   variable and pair of scenarios for each day in the calendar year through 2100.

142   Because of Rio de Janeiro's complex coastal and mountainous terrain, projections may
143 not accurately capture fine scale differences in the city's climate. For example, recent literature
144 has shown that the coastal cooling relative to inland areas experienced in regions such as the
145 eastern United States may be underestimated by global climate models (Raymond and Mankin
146 2019). These biases are greatest in regions with large land-ocean surface temperature contrasts,
147 however, and Rio de Janeiro's location in the tropics, as well as the fact that the extreme events
148 analyzed in this study take place in the spring when this temperature gradient should be
149 relatively small, may mute these biases compared to other regions and seasons. In order to
150 address these potential sources of error, we generate a set of synthetic time series based on
151 NEXGDDP projections which retain the seasonality and variability recorded in the historical
152 reanalysis data from ERA5. We use a percentile matching technique in which we first bin all
153 data for the grid cell which includes the city of Rio de Janeiro during a historical base period
154 (1981-2013) into one-percentile bins for both the NEXGDDP and ERA5 datasets. We
155 additionally bin all NEXGDDP data from this grid cell into one-percentile bins during one
156 midcentury period (2041-2060) and one end-of-century period (2081-2100). We then calculate
157 the temperature delta for each percentile bin between the base period and both the midcentury
158 and the end-of-century periods in the NEXGDDP data. Finally, we add these percentile-specific
159 change factors to every data point in each associated bin in the historical ERA5 base period.
160

161 **2.2 Methodology**
162   We first create time series for the historical day-of-year climatologies of variables in the
163 city of Rio de Janeiro and compare them to the evolution throughout 2023. All anomalies are
164 calculated relative to historical mean calendar date values (i.e., the daily maximum temperature
165 anomaly on November 18, 2023 is calculated by subtracting the mean daily maximum
166 temperatures on November 18 in all previous years in the historical record from the recorded
167 absolute magnitude of the event). We also generate maps of concurrent meteorological variables
168 relevant to the extreme heat event for the greater region outside of Rio de Janeiro. We compare
169 these spatial patterns to those experienced during previous extreme heat events in Rio de Janeiro,
170 calculated as 99th percentile daily maximum temperature days across all seasons for the grid cell
171 which includes the Galeão International Airport weather station. We then select for events that
172 occur in the September-November (SON) austral spring season.

Deleted: data

Deleted: However, models are particularly biased

Deleted: as

Deleted: a tropical city and

Deleted: suggest that these

Deleted: may be muted

Deleted: apply

Deleted: percentile

Deleted: each

Deleted: which

Deleted: only

184   We also quantify how extreme heat in the city of Rio de Janeiro is shifting using a variety

185 of methods. We first calculate the trend in the frequency of extreme temperatures over the

186 historical record in Brazil, defining these extreme temperatures using both absolute and relative

187 thresholds. We select these thresholds as 30°C and the locally defined 90th percentile daily

188 maximum temperature at each grid cell. These thresholds are chosen in order to investigate

189 impactful temperature magnitudes while ensuring sufficient sample size for the trend analysis.

190   We also visualize the broadening of the extreme heat season, calculated based on the

191 number of days between the start of the first heatwave and end of the last heatwave of the

192 season. A heatwave is defined here as a three-day period with consecutive daily maximum

193 temperatures above the 50th percentile of daily maximum temperatures across the two hottest

194 months of the year in the city of Rio de Janeiro (January and February); this 50th percentile

195 threshold is equal to about 31.4°C. This heat season definition is informed by a definition used

196 by the United States Environmental Protection Agency (US EPA 2021), adapted to better reflect

197 Rio de Janeiro's lower temporal variability in temperature due to its tropical location.

198   Finally, we calculate how spring temperature distributions have already changed in Rio

199 de Janeiro by comparing early and late historical periods in ERA5 for the grid cell which

200 includes the Galeão International Airport weather station. Distributions are calculated from

201 annual spring maximum temperatures in the city of Rio de Janeiro and fit using GEV

202 distributions, which have been shown to well capture extreme temperature distributions (Powis

203 et al., 2023; Van Oldenborgh et al., 2022). For comparison, we also plot GEV distributions for

204 early and late historical periods in the NEXGDDP model data before applying our bias-

205 correction technique. The location parameter and spread of the model data distributions during

206 these periods is much lower than that of ERA5 (Fig. S2), further motivating our use of synthetic

207 time series to explore how these distributions may change in the future.

208   We then use the bias-corrected NEXGDDP data for the 23 models which report daily

209 maximum temperature for each day in the calendar year under the aforementioned SSP2-4.5 and

210 SSP5-8.5 scenarios during a midcentury and end-of-century time period. We additionally

211 evaluate the impact of only using models which most accurately reproduce the historical

212 observed daily maximum temperature record in the city of Rio de Janeiro. We calculate the

213 Perkins skill score to evaluate the similarity between probability density functions of daily

214 maximum temperature in the reanalysis dataset (ERA5) and each of the 23 global climate models

219 during the historical period. These skill scores are calculated as the cumulative minimum
220 between the observed and modeled distributions of each binned value (Perkins et al., 2007). We
221 finally select the 6 climate models which exhibit skill scores greater than 0.8, indicating that
222 these models capture over 80% of the observed probability density functions. The result of this
223 analysis is shown in Fig. S3, but the interpretation of the results as shown in the main text using
224 all 23 models does not change.
225
226 **3 Results**
227 **3.1 Rio de Janeiro's spring 2023 heatwave**
228   The city of Rio de Janeiro experienced exceptionally high temperatures in both the
229 austral winter and spring of 2023, peaking on November 18 (Fig. 1). This record-breaking event
230 became the highest daily maximum temperature on record at the Galeão International Airport
231 weather station, reaching 41.3°C. The extreme heat event was also notable for its accompanying
232 high specific humidity, which rose alongside temperature in the days leading up to November 18
233 (Fig. 1b). The combination of elevated temperature and humidity rendered the event a humid
234 heat extreme, as measured by wet bulb temperature, which peaked at 28.2°C on November 18
235 (Fig. 1c). The coincidence of extreme dry and wet bulb temperatures is typical for extreme heat
236 events in Rio de Janeiro, where there is a statistically significant positive correlation between
237 daily maximum temperature and daily mean specific humidity (Fig. S4). This relationship is
238 facilitated by the city's abundant access to moisture from the coast and surrounding vegetation.
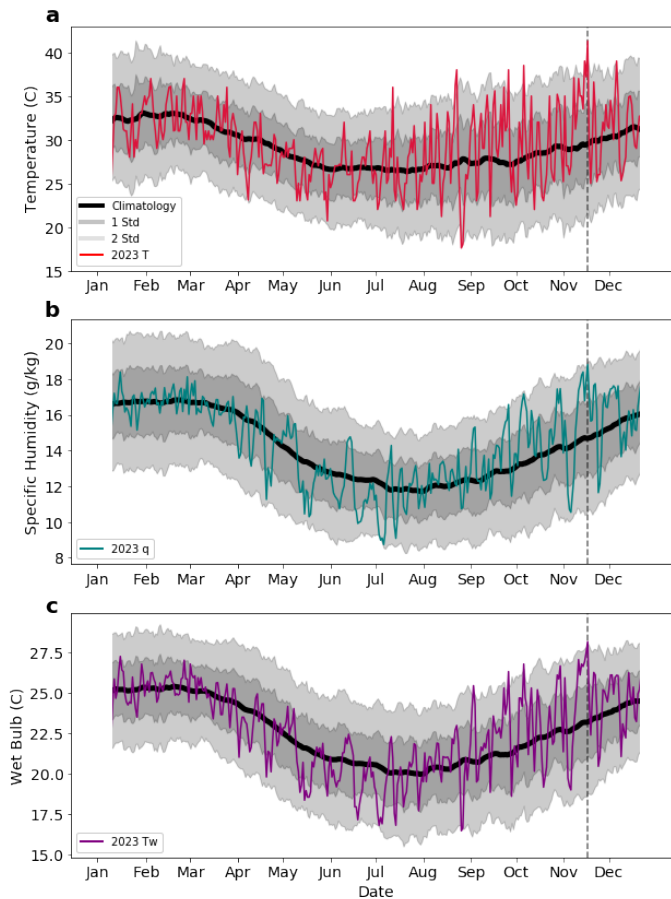
Figure 1: Historical climatology and 2023 recorded a) daily maximum temperature, b) daily mean specific humidity, and c) daily maximum wet bulb temperature in the city of Rio de Janeiro. Data from the Galeão International Airport weather station as reported by the HadISD dataset. Vertical dashed line identifies record-breaking temperature event on November 18, 2023.

Elevated temperatures occurred over an area greater than the city of Rio de Janeiro, but were spatially constrained by orography (Fig. 2). We explore the spatial patterns of the heatwave in data from the European Centre for Medium-Range Weather Forecasts (ERA5) reanalysis during the period of 1979-2023 (Hersbach et al., 2020). We see that hotspots in elevated

> **Deleted:** were not limited to the city of
>
> **Deleted:** elevation

252 temperatures were located throughout the coastal region surrounding Rio de Janeiro, with sharp

253 declines across the mountainous terrain moving inland. These positive coastal temperature

254 anomalies coincide with northerly surface wind anomalies. ERA5 estimates the daily maximum

255 temperature on November 18 in the grid cell containing the Galeão International Airport weather

256 station as 40.6°C, within the range of temperatures recorded throughout weather stations in the

257 city (Fig. S1). This extreme event was also remarkable in length as measured by ERA5, as daily

258 maximum temperatures were above the locally defined 90th percentile for eight consecutive days,

259 and above the 99th percentile for the final three days of this period (percentiles calculated from

260 ERA5 across the period from 1979-2023). This multi-day interval of exceptional temperatures

261 rendered it difficult for residents to find relief.

262
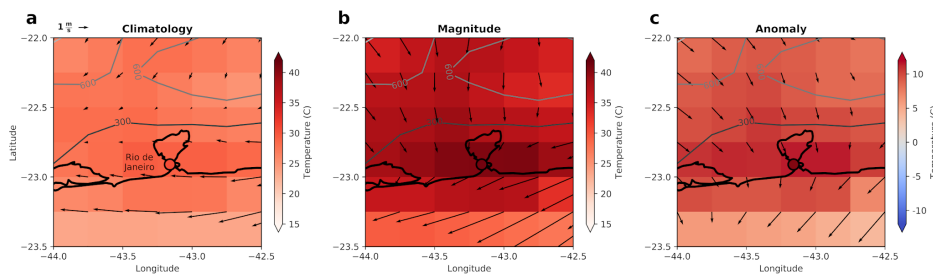
263 **Figure 2: Spatial maps of daily maximum temperatures during the date of peak extreme**
264 **heat intensity in the city of Rio de Janeiro using ERA5 data (shading) and the Galeão**
265 **International Airport weather station (marker). Vectors represent surface winds; contours**
266 **represent elevation in meters. A) Climatology during November 18 throughout the**
267 **historical record. B) Magnitudes on November 18, 2023. C) Anomalies during November**
268 **18, 2023.**

269

270 The maximum temperature during the event on November 18 coincided in time with

271 other anomalous meteorological conditions (Fig. 3; for climatological values, see Fig. S5 in the

272 Supplemental Materials). Positive geopotential height anomalies centered over Rio de Janeiro

273 were consistent with an intensification of the South American Subtropical High, a semi-

274 permanent anticyclonic circulation system off the Southeast coast of Brazil. The edge of this

275 positive high pressure anomaly was collocated with the region of positive temperature anomalies

276 that includes the city of Rio de Janeiro. Surface winds off the coast of Rio de Janeiro were

277 anomalously northerly. Previous literature has shown that such anomalously northerly winds

280 over the coast can increase local sea surface temperatures through reductions in wind-driven

281 upwelling, reducing the capacity for coastal cooling (Castelao and Barth 2006; Palma and

282 Matano 2009). Further, anomalously northerly flow in this mountainous area can exacerbate high

283 temperatures directly through downslope winds (Stefanello et al. 2022). Anomalous winds over

284 the interior of South America also enhanced the northerly South American Low Level Jet

285 (Marengo et al., 2004; Montini et al., 2019). Positive specific humidity anomalies were present

286 throughout Southeast and South Brazil, intersecting with an area of precipitation along the edge

287 of the low pressure system to the south. The northern portion of the positive specific humidity

288 anomaly was aligned with the positive geopotential height anomaly off the coast of Southeast

289 Brazil. Widespread negative soil moisture anomalies occurred throughout most of Brazil, and the

290 interior of South America more broadly, during this event. The large spatial coverage of these

291 negative soil moisture anomalies was concurrent with Amazonian drought recorded during this

292 time, inherited from the prior season (Espinoza et al., 2024). Finally, positive SSTs of up to 2°C

293 occurred along Rio de Janeiro's coast. These spatial patterns are typical of extreme heat events

294 during the spring season in the city of Rio de Janeiro, though the magnitudes of the anomalies in

295 all of these variables are dramatically higher on November 18, 2023 than during other spring

296 extreme heat events (Fig. 4). The most unique features of the November 18 event were the

297 intensified northerly winds and the degree of inland penetration of positive specific humidity

298 anomalies. Further, the positive local SST anomalies off the coast of Rio de Janeiro were

299 particularly exceptional in intensity and spatial scale during this event, weakening the sea-air

300 temperature contrast and sea-breeze. Outside of these specific distinctions, the event on

301 November 18, 2023 was an intense example of a typical spring extreme heat event in the region.

304
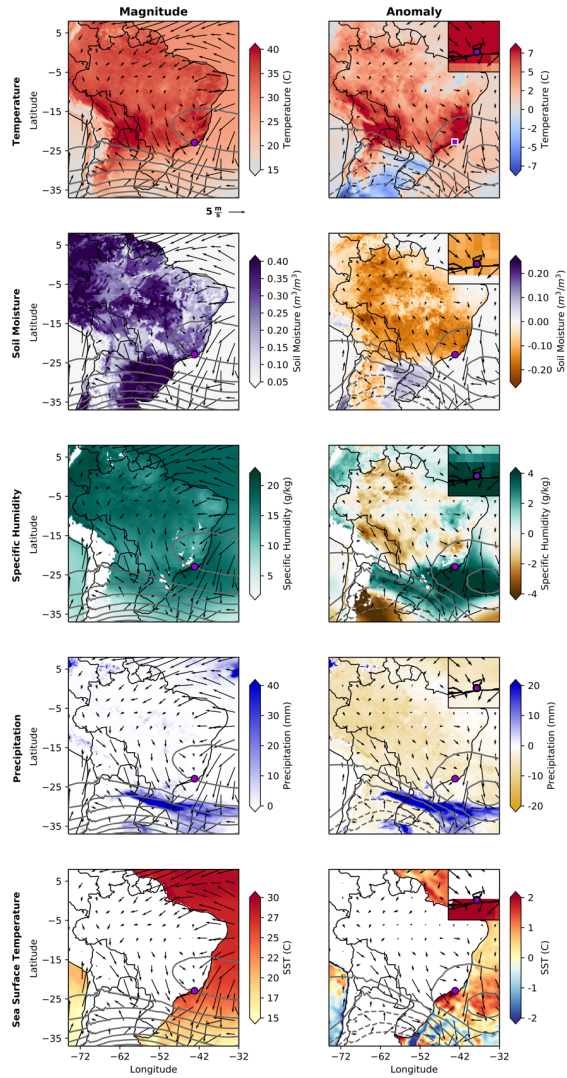
Figure 3: Magnitude (left) and anomalies (right) of daily maximum temperature, mean soil moisture, mean specific humidity, total precipitation, and mean SST on day of peak temperature in the city of Rio de Janeiro (November 18, 2023). Overlying wind vectors and 500 hPa geopotential height contours (50 m and 25 m contour levels for magnitude and anomaly plots, respectively). Anomalies calculated relative to historical calendar date mean values across the period from 1979-2023. Inset in the upper right corner of each anomaly

plot zooms in on the white box surrounding the city of Rio de Janeiro (purple marker) in the top right subplot.
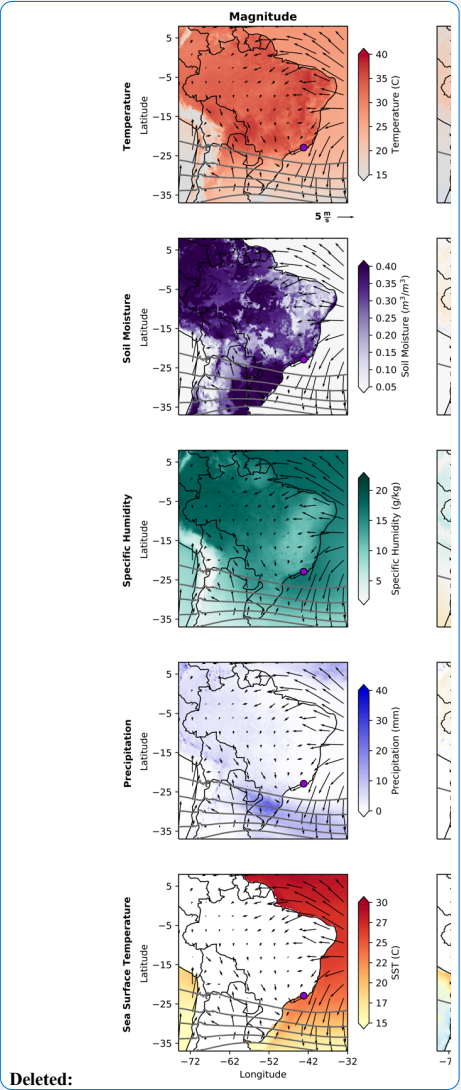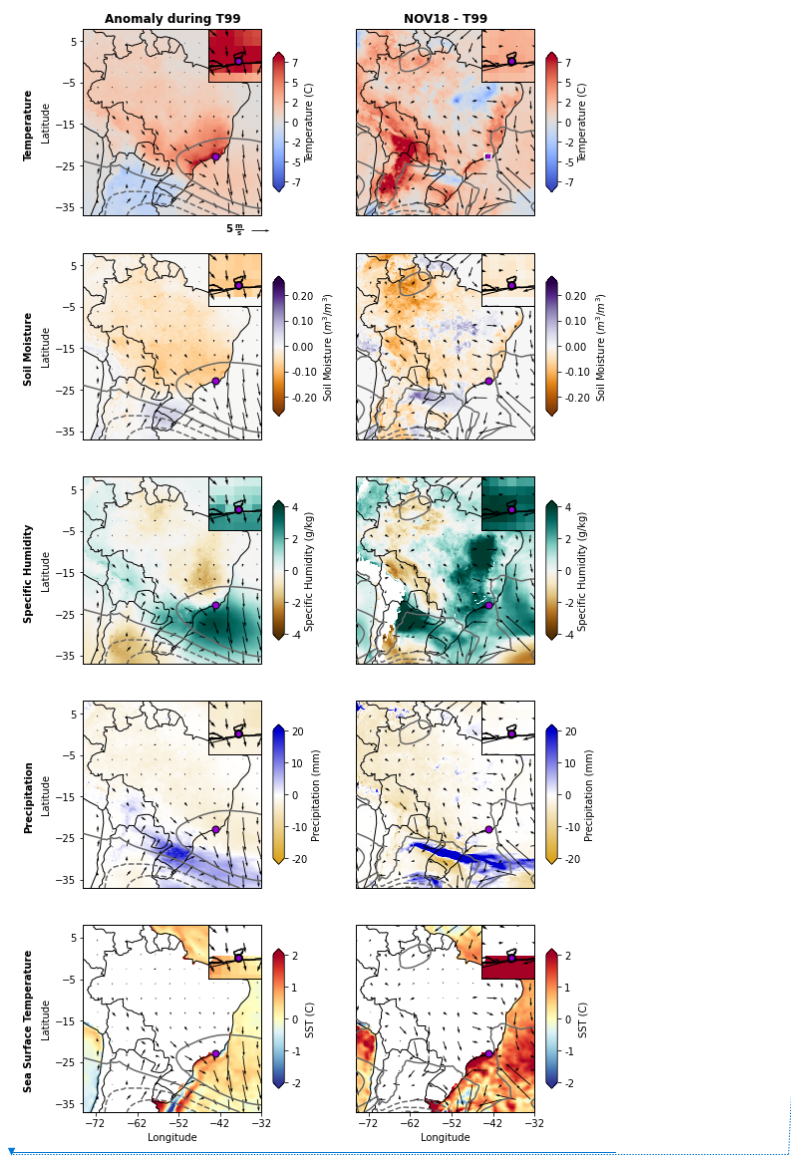
Deleted:

Figure 4: Anomalies in daily maximum temperature, mean soil moisture, mean specific humidity, total precipitation, and mean SST during 99th percentile extreme temperature days in the September-November (SON) season for the ERA5 grid cell which includes the Galeão International Airport weather station (left). Difference in conditions on November 18 compared to mean conditions during these 99th percentile extreme temperature days (right).

The time evolution of the meteorological variables described above throughout the month of November 2023 uncovers the temporal development of the extreme heat event (Fig. 5). Rising temperatures throughout the weeks leading up to November 18 were preceded by elevated geopotential heights at 500 hPa and associated atmospheric subsidence. This was accompanied by a rapid decline in soil moisture which was likely facilitated by the increased solar insolation associated with the persistent high pressure system and resulting extremely low precipitation from November 2-November 18. Given that the rainy season in Southeast Brazil typically begins in late-October to mid-November (Coelho et al., 2021; Latinovic et al., 2018; Marengo et al., 2012; Liebmann and Mechoso 2011; Raia and Cavalcanti 2008), this period of consecutive dry days was unusual. Indeed, this period totals 17 days in a row with less than 5 mm of rain per day, and this only happened during the month of November in one other year in the historical record from ERA5 between 1979-2023 (2012). These changes in geopotential height, soil moisture, and suppressed precipitation preceded changes in other variables, evidenced by the grey lines in the background of each subplot. There was also a gradual increase in SST off the coast of Rio de Janeiro, though delayed compared to that of the local air temperature. Wind direction was highly variable on a daily scale, but became increasingly northerly during this same period. As air temperatures rose, specific humidity increased over the city. This was likely related to both local evaporation from the soil (co-occurring with declining soil moisture) and moisture advected from the coast and surrounding vegetation. The circulation specifically on November 18 directed wind in the larger region surrounding Rio de Janeiro to intensify the South American Low Level Jet, which can additionally increase moisture transport from the Amazon Basin to Southeast Brazil (Marengo et al., 2004; Vera et al., 2006; Montini et al., 2019). However, convergence of the horizontal moisture flux at the level nearest the surface was only stronger than its climatological values in some grid cells within the northern and western areas of the city (Fig. S6). More generally, specific humidity was also able to build without reaching saturation due to the increasing temperatures (and the Clausius-Clapeyron relation). Finally, the heatwave was

355 terminated when a two-day precipitation event occurred from November 19- 20. This

356 precipitation induced a small decline in specific humidity and SST, as well as a rapid increase in

357 soil moisture.

358
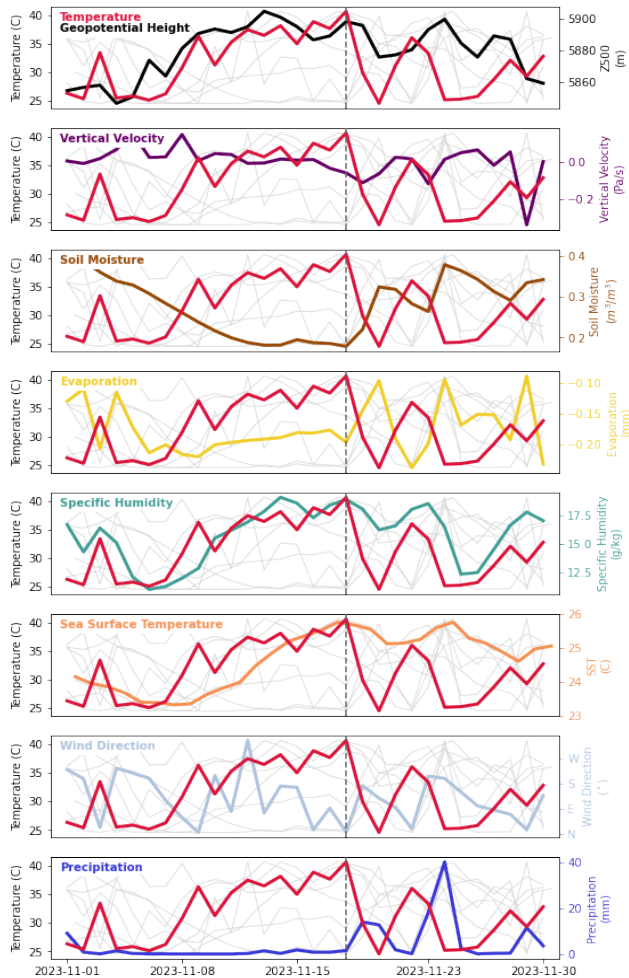
Figure 5: Evolution of meteorological conditions during the month of November 2023 in Rio de Janeiro. Grey lines in the background of each subplot show the evolution of all variables, with individual variables compared in colors to dry bulb temperature in red. Vertical dashed line identifies record-breaking temperature event on November 18, 2023. All variables are calculated for the grid cell which includes the Galeão International

364 **Airport weather station except SST, which is averaged over the box 21°S-24°S and 42°W-**
365 **45°E.**

366

367 The evolution of the 2023 heatwave as shown above is reminiscent of that during the

368 2010 heatwave analyzed by Geirinhas and coauthors (2019). Those authors explain that the

369 extreme heat event in the summer of 2010 was initiated by a positive SST anomaly over the

370 eastern Pacific that triggered a Rossby wave train that in turn intensified the South Atlantic

371 Subtropical High. Modulation of this climatological high pressure system has been shown to be

372 central to influencing weather in the city of Rio de Janeiro, and particularly temperatures there

373 (Geirinhas et al., 2018). Here we also observe a positive SST anomaly over the equatorial Pacific

374 throughout the month of November and a resulting anomalous wave pattern ending over the

375 South Atlantic High that became increasingly organized and strengthened during the two weeks

376 before November 18 (Fig. 6; see Fig. S7 in the Supplemental Materials for maps of the

377 climatologies and absolute magnitudes of these variables). This mechanism is similar to how El

378 Niño generally influences temperatures in Southeast Brazil on longer timescales (Cai et al.,

379 2020), and we confirm that there is a positive correlation between the ENSO state as quantified

380 by the Niño3.4 index and the frequency of high heat days in the city of Rio de Janeiro in the

381 austral spring season (Fig. S8). Further, the mean spatial SST and Z200 patterns during the

382 spring of typical El Niño years look very similar to those observed during November 2023,

383 though the anomalies in both SST and geopotential height are much larger during November

384 2023 (Figure S9). 2023 was characterized by a transition from La Niña to El Niño, with the El

385 Niño emerging in April-June 2023 and strengthening to a strong El Niño in the second half of

386 2023 (Becker et al., 2024). The SST anomalies associated with the El Niño could have been

387 responsible for initiating the wave train which set off the geopotential height anomalies over Rio

388 de Janeiro. We note that similar wave trains driven by Pacific SST anomalies have been shown

389 to influence weather in Southeast Brazil even during neutral ENSO states (Seth et al., 2015).

390 Additionally, the instantaneous extreme temperature event and the preceding persistent dry

391 conditions must also be linked to the synoptic weather in the area. Decreases in soil moisture and

392 horizontal moisture fluxes by intensification of the South American Low Level Jet were central

393 features of the heatwave in 2010, as they were in November 2023. These overlaps in the apparent

394 drivers of the 2010 and 2023 heatwaves underscore that while last year's spring event was

Deleted: n

Deleted: n

Deleted: conditions

Deleted: occurrence of

Deleted: conditions

Deleted: from

Deleted: anomalous winds

Deleted: to the development of the

unprecedented in its magnitude and unusual in its spring timing, it was not unique in its overall dynamics.
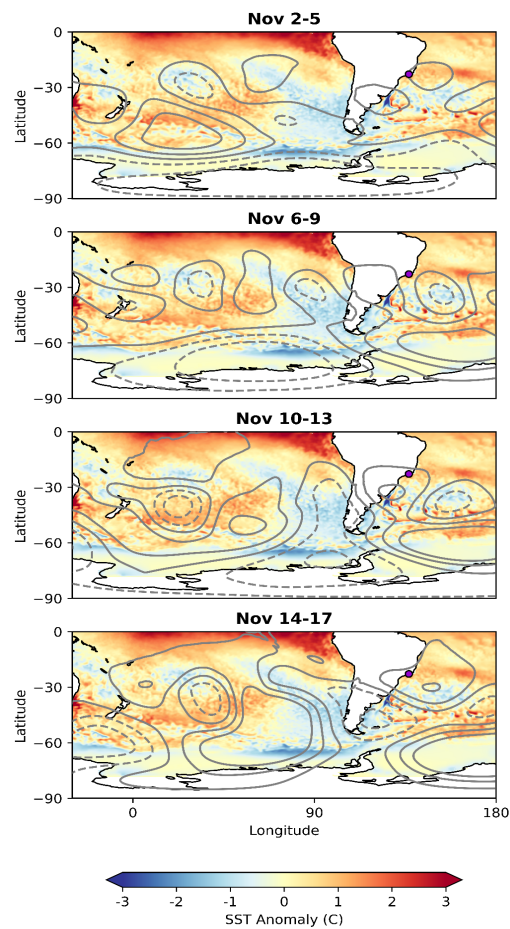
Figure 6: Evolution of the geopotential height at 200 hPa (contours) in the weeks of suppressed precipitation leading up to the extreme heat event on November 18 in the city of Rio de Janeiro. Geopotential height anomaly contour levels are at 100 m, with positive (negative) anomalies in solid (dashed) contours. Across all subplots, shading indicates November 2023 mean SST anomalies.

3.2 Historical and future changes in extreme heat

413   Extreme heat events have become more frequent in the city of Rio de Janeiro and the
414   timing of these events has shifted earlier in the calendar year. There has been a significant
415   increase in the number of days above 30°C each year over the past 44 years throughout almost
416   all of South America (Fig. 7a). Further, the number of 90th percentile days locally defined at each
417   grid cell has also increased significantly throughout most of the region (Fig. 7b). In the city of
418   Rio de Janeiro specifically, the number of 30°C days per year during the austral spring is
419   increasing at a rate of 0.27 days/year (Fig. 7c). Relative to 1979, the city now experiences almost
420   12 additional days per year above 30°C during the spring season alone. Overall, the extreme heat
421   season in Rio de Janeiro is broadening. As measured by the number of days between the first and
422   last heatwave day of the season (a period of three or more consecutive days with daily maximum
423   temperatures above 31.4°C), the extreme heat season has lengthened from 156 days in the 1979-
424   1980 season to 176 days in the 2022-2023 season (Fig. 8). The broadening of the heat season is
425   due primarily to more early season heatwave days, while the end date of the heat season has not
426   changed significantly.
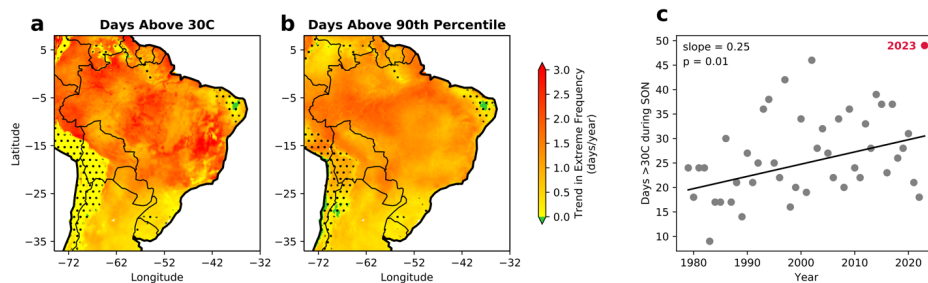
427
428   **Figure 7: Historical trend from 1979-2023 in the number of days per year above a) 30°C**
429   **and b) locally defined 90th percentile. Stippling shows areas which are not significant at a p**
430   **= 0.05 level assessed using a Wald Test. c) Trend in number of days per year above 30°C**
431   **taking place in the SON season in ERA5 for the grid cell which includes the Galeão**
432   **International Airport weather station.**

433

437
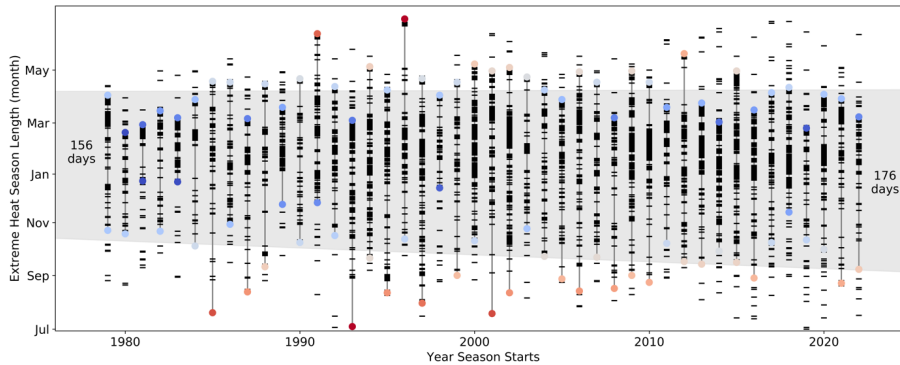
Figure 8: Shifting timing of the city of Rio de Janeiro extreme heat season. Horizontal axis
indicates the year in which winter begins ("January" marking denotes the start of the
following calendar year). Colored markers indicate the first and last days of the extreme
heat season each year. Marker color indicates whether the start/end date is lengthening
(red) or shortening (blue) the heat season compared to historical mean start/end dates.
Dashes indicate individual additional days with daily maximum temperatures surpassing
31.4°C (no persistence required). Grey shading indicates area between trend lines in the
shifting seasonality.

446

The distribution of maximum spring temperatures in the city of Rio de Janeiro has shifted

higher over the last four decades and this pattern is projected to continue in the future. In order to

evaluate whether the observed historical increase in extreme heat frequency identified in Figures

7 and 8 may continue in the future, we fit annual maximum spring temperatures from historical

ERA5 reanalysis data and future projections from bias-corrected NASA Earth Exchange Global

Daily Downscaled Projections (NEXGDDP) data (Thrasher et al., 2022, see Methods) to a

Generalized Extreme Value (GEV) distribution. When comparing early and late historical

periods from 1979-1988 and 2014-2023, respectively, the location parameter of the two GEV

distributions has increased by 1.7°C (Fig. 9). The distribution of maximum austral spring

temperatures in the city of Rio de Janeiro is also projected to continue shifting to higher values in

the future, but the magnitude of this change is strongly dependent upon the future emissions

pathway. The temperature distributions associated with mid-century periods (2041-2060) under

SSP2-4.5 and SSP5-8.5 future scenarios are similar to that of the last 10 years of observational

data, with shifts in the location parameters of 0.1°C and 0.9°C for the two emissions trajectories,

466 respectively. A larger change is projected by the end of the century (2081-2100) under each
467 emissions scenario. However, the end-of-century SSP5-8.5 scenario is distinctly separate from
468 the other distributions, with the distribution location parameter 2.8°C higher than during the last
469 10 years.
470   These changes to the distributions strongly influence the probability of an event with the
471 intensity of the maximum temperature recorded on November 18, 2023. The probability density
472 function fit to the projected annual maximum spring temperatures under each mid-century period
473 using a GEV distribution yields a return period for an extreme temperature event with the daily
474 maximum temperature at least 40.6°C in the city of Rio de Janeiro (analogous to the event on
475 November 18, 2023 as measured by ERA5) of 51 years under SSP2-4.5 and 33 years under
476 SSP5-8.5. By the end of the century under either emissions scenario, an event of this magnitude
477 becomes much more likely, with return periods of 19 years or just 4 years under SSP2-4.5 and
478 SSP5-8.5, respectively. Recent literature has suggested that the SSP5-8.5 scenario may not be
479 realistic given our current socioeconomic, political, and physical landscape (Hausfather and
480 Peters 2020; Burgess et al., 2020; Ritchie and Dowlatabadi 2017). However, these results
481 indicate that an austral spring heatwave of the magnitude experienced in the city of Rio de
482 Janeiro on November 18 is projected to become much more frequent in the future, even under
483 the more stringent SSP2-4.5 emission pathway. We must also note that it is difficult to evaluate
484 whether the models are missing emerging factors that could increase the frequency and intensity
485 of these extreme heat events – such as Amazonian deforestation or declines in sea ice – reducing
486 their ability to capture the possible future spring temperature distributions in Rio de Janeiro.
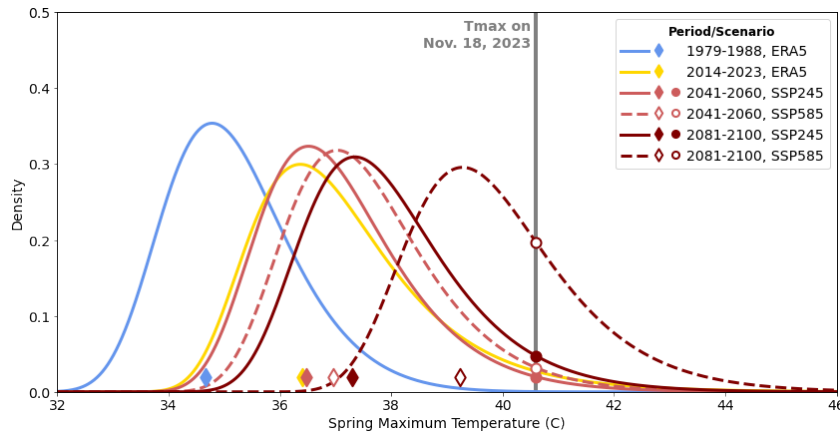
Figure 9: Generalized Extreme Value distributions for SON maximum temperatures during early and late historical periods (observed in ERA5), mid-century periods, and end-of-century periods under SSP2-4.5 and SSP5-8.5 (projections from bias-corrected NEXGDDP data). Diamonds indicate the value of the location parameter for each distribution. Vertical grey line shows the magnitude of the extreme temperature event on November 18, 2023.

4 Conclusions

The November 2023 heatwave in the city of Rio de Janeiro was a record-breaking event characterized by meteorological conditions largely typical of spring extreme temperature events, but exceptional in their magnitudes. Rising temperatures were associated with positive geopotential height anomalies and corresponding atmospheric subsidence which facilitated clear sky conditions and increased sensible heat flux at the surface. These high pressure anomalies centered over the South Atlantic Subtropical High were likely related to the strong 2023-24 El Niño event. The subsidence near Rio de Janeiro associated with the geopotential height anomalies also suppressed precipitation and facilitated evaporation from the land surface, leading to decreased soil moisture and increased specific humidity. Moisture was available from multiple sources to facilitate these humidity increases, as Rio de Janeiro is a coastal city and downwind of both the Amazon and more local vegetation. SSTs off the coast of Rio de Janeiro were also highly elevated in the days before the heatwave peak, reducing the potential for coastal cooling. Finally, the event was terminated on November 19 due to the evaporative cooling, shading, and

510 mixing associated with the onset of precipitation. The combination of changes in circulation,

511 land surface feedbacks, and atmosphere-ocean interactions generated the conditions for an

512 exceptionally intense and persistent extreme heat event in the city of Rio de Janeiro.

513 The risk of extreme heat in austral spring is increasing significantly in Rio de Janeiro. We

514 find that extreme spring temperature events are becoming more frequent and that the extreme

515 heat season is starting earlier and lasting longer than in previous decades. Further, extreme heat

516 of the magnitude on November 18, 2023 may become much more likely by mid- and end-of-

517 century periods. However, the absolute increase in the frequency of similar heatwaves is largely

518 dependent upon our future emissions pathway.

519 The November 2023 heatwave had devastating impacts, including loss of life. As our

520 climate continues to change and extreme heat in the city of Rio de Janeiro continues to increase

521 in intensity and frequency, we can expect more strain on human health and cascading

522 socioeconomic impacts. This extreme heat event was exceptional not only in its intensity, but

523 also in its persistence. Consecutive extreme heat days have been shown to have nonlinear

524 impacts on human health, in Brazil and in other countries, as they prevent individuals, buildings,

525 and critical electrical equipment from cooling down between heat events (Geirinhas et al., 2020;

526 Baldwin et al., 2019). More broadly, the direct impacts of heatwaves on hospitalizations

527 throughout Brazil have been documented, with the largest effects occurring in long duration

528 events (Zhao et al., 2019). These impacts of heatwaves on mortality are projected to increase,

529 with particular consequences for elderly populations, especially if targeted adaptation measures

530 are not put in place (Diniz et al., 2020). Continuing to improve our understanding of how and

531 when extreme heat occurs is thus essential as our climate continues to change. This is

532 particularly true for locations such as Rio de Janeiro, which historically has not been a hotspot of

533 extreme heat – especially in the shoulder seasons – and thus individuals may not be well

534 acclimated to extreme temperatures then (Periard et al., 2015; Horowitz 2016). The human health

535 impacts of unusually intense events may be exacerbated by the shifting timing of extreme heat,

536 as record-breaking exceptional heat events are now occurring outside of the traditional extreme

537 heat season when individuals may not be prepared to utilize heat mitigation strategies (De Freitas

538 & Grigorieva, 2015). Because Rio de Janeiro is an area of emerging risk for extreme heat, further

539 research on models' ability to capture the historical drivers and timing of heatwaves in this

540 region and evaluations of how these characteristics might shift in the future should be pursued.

544   The meteorological conditions surrounding the extreme heat event analyzed here

545   demonstrate the potential for compound hazards throughout Brazil. The identified circulation

546   pattern that establishes the atmospheric blocking associated with heatwaves in Rio de Janeiro is

547   also likely linked to heavy precipitation events in South Brazil, an extreme case of which

548   occurred in May 2024 in center-north of Rio Grande do Sul, including the metropolitan area of

549   Porto Alegre, displacing hundreds of thousands and killing at least 155 people (Rogero 2024).

550   The temporal compounding of these extreme temperature and flooding events within Brazil has

551   the potential to strain the country's disaster management systems more than events occurring in

552   isolation. Furthermore, the exceptional spatial area within Brazil that experienced anomalous

553   heat in the November 2023 event, relative to 99th percentile heat events in the city of Rio de

554   Janeiro, underscores the potential for spatially compounding heat that could lead to outsized

555   impacts. Exploring how unprecedented global surface ocean and surface temperatures, along

556   with regional features like the broader heat and drought across much of Brazil, may contribute to

557   extreme heat in the city of Rio de Janeiro will be an important component to improving our

558   understanding of these compound events' drivers, prediction capacity, and potential to change in

559   the future.

560   The evolving meteorological conditions associated with this heatwave were strongly

561   impacted by the lack of precipitation in the first two weeks of November. This is particularly

562   unexpected due to the fact that the active phase of the South American Monsoon System

563   typically begins in late October or early November in this region (Marengo et al., 2012;

564   Liebmann and Mechoso 2011; Raia and Cavalcanti 2008), which is linked to an increase in

565   convective activity in tropical South America in the warm season (Jones and Carvalho 2013).

566   Observational and modeling studies suggest that the South American Monsoon System dry

567   season is lengthening (Arias et al., 2015; Fu et al., 2013) and that the onset of the active phase is

568   delaying (Gomes et al., 2022; Pascale et al., 2019). These trends are projected to continue to

569   some degree in the future with further climate change, particularly in light of ongoing

570   deforestation which contributes to regional drying trends in the Amazon and other areas of Brazil

571   (Boisier et al., 2015; Swann et al., 2015). Given Rio de Janeiro is a city with abundant access to

572   moisture due to its proximity to the coast and vegetation, the increasingly constrained active

573   monsoon phase could lead to increased frequency and intensity of extreme humid heat in the

574   spring season (Ivanovich et al., 2024). These changes could be responsible for the evident

576 asymmetrical historical increase in heat season length during the spring versus fall as
577 demonstrated here, and extensions of this work should be devoted to an exploration of these
578 potential relationships.
579   This work highlights the challenge of analyzing the drivers of weather extremes in such a
580 climatically diverse city as Rio de Janeiro and emphasizes the need for future research to explore
581 high resolution comparisons of mechanisms controlling the city's microclimates. Differences
582 between conditions recorded at individual weather stations within the city's boundaries
583 demonstrate the degree to which the dynamics of events in each neighborhood depend on the
584 station's location relative to the coast versus interior (Raymond and Mankin 2019), elevation
585 (Raymond et al., 2022; Pepin et al., 2015), and degree of urbanization (Kruger et al., 2024;
586 Chakraborty et al., 2022; Tan et al., 2010). Higher temporal resolution analysis would also better
587 capture sub-daily processes such as sea breeze and their effect on extreme heat throughout the
588 city. Further, many of these mechanisms influencing the intracity variability of heat stress
589 exposure only focus on the effect of differences in dry bulb temperature. Factoring in the spatial
590 variation in humidity, solar insolation, and windspeed complicate understanding, but are
591 essential for capturing humans' exposure to heat stress conditions. These intracity differences
592 also meaningfully impact compound events with non-heat environmental hazards, such as floods,
593 landslides, droughts, and air pollution, as well as how exposure to these hazards intersects with
594 areas of social vulnerability. Future work should be devoted to investigating the different
595 magnitudes of extreme heat and controlling mechanisms throughout Rio de Janeiro in order to
596 inform targeted extreme heat adaptation plans for individual neighborhoods within the city.
597
598 *Data Availability:* The publicly available datasets used in this analysis are accessible via the
599 following websites: HadISD, https://www.metoffice.gov.uk/hadobs/hadisd/; ERA5,
600 https://cds.climate.copernicus.eu/datasets/reanalysis-era5-single-levels?tab=overview and
601 https://cds.climate.copernicus.eu/datasets/reanalysis-era5-pressure-levels?tab=overview; OISST,
602 https://www.ncei.noaa.gov/products/optimum-interpolation-sst; and NEXGDDP,
603 https://www.nccs.nasa.gov/services/data-collections/land-based-products/nex-gddp-cmip6.
604 Station data from the Rio Alert System will be uploaded and accessible via a GitHub repository
605 upon manuscript publication.
606

Code Availability: All code used for the derivations, calculations, and data visualization will be made publicly available via a GitHub repository upon manuscript publication.

Author Contributions:

S.J.C. conceived of the initial project concept. All co-authors contributed to study design, and C.I. performed the analysis. C.I. wrote the initial manuscript draft with the feedback and interpretation of all co-authors. All co-authors read and edited the manuscript.

Competing Interests:

The authors declare that they have no conflict of interest.

Acknowledgements:

This work was partially supported and funded by Columbia Global at Columbia University, "Simulation of Extreme Weather Events in Brazilian Megacities", a Climate Hub | Rio Project. Climate Hub | Rio is a knowledge, research, and innovation hub that brings together experts from Brazil, Columbia University, and around the world to advance climate-related knowledge and action in Rio and Brazil. Direct funding for C. Ivanovich and R. Horton was provided by National Oceanic and Atmospheric Administration's Regional Integrated Sciences and Assessments program, Grant NA15OAR4310147. A. H. Sobel acknowledges support from NSF Grant AGS-1933523. S. J. Camargo is partially supported by the NOAA grant NA23OAR43201600. The authors declare no competing interests.

References

Alvares, C. A., Stape, J. L., Sentelhas, P. C., & De Moraes Gonçalves, J. L. (2013). Modeling monthly mean air temperature for Brazil. Theoretical and Applied Climatology, 113(3–4), 407–427. https://doi.org/10.1007/s00704-012-0796-6

Alvarez, M. S., Vera, C. S., Kiladis, G. N., & Liebmann, B. (2016). Influence of the Madden Julian Oscillation on precipitation and surface air temperature in South America. Climate Dynamics, 46(1), 245–262. https://doi.org/10.1007/s00382-015-2581-6

Arias, P. A., Fu, R., Vera, C., & Rojas, M. (2015). A correlated shortening of the North and South American monsoon seasons in the past few decades. Climate Dynamics, 45(11), 3183–3203. https://doi.org/10.1007/s00382-015-2533-1

Baldwin, J. W., Dessy, J. B., Vecchi, G. A., & Oppenheimer, M. (2019). Temporally Compound Heat Wave Events and Global Warming: An Emerging Hazard. Earth's Future, 7(4), 411–427. https://doi.org/10.1029/2018EF000989

Becker, E., L'Heureux, M., Hu, Z.-Z., & Kumar, A. (2024). ENSO and the tropical Pacific. In "State of the Climate in 2023". *Bull. Amer. Meteor. Soc.*, 105 (8), S221-S224, https://doi.org/10.1175/BAMS-D-24-0098.1

Bitencourt, Daniel P., Fuentes, M. V., Franke, A. E., Silveira, R. B., & Alves, M. P. A. (2020). The climatology of cold and heat waves in Brazil from 1961 to 2016. International Journal of Climatology, 40(4), 2464–2478. https://doi.org/10.1002/joc.6345

Bitencourt, Daniel Pires, Muniz Alves, L., Shibuya, E. K., De Ângelo Da Cunha, I., & Estevam De Souza, J. P. (2021). Climate change impacts on heat stress in Brazil—Past, present, and future implications for occupational heat exposure. International Journal of Climatology, 41(S1). https://doi.org/10.1002/joc.6877

Boisier, J. P., Ciais, P., Ducharne, A., & Guimberteau, M. (2015). Projected strengthening of Amazonian dry season by constrained climate model simulations. Nature Climate Change, 5(7), 656–660. https://doi.org/10.1038/nclimate2658

Burgess, M. G., Ritchie, J., Shapland, J., & Pielke, R. (2020). IPCC baseline scenarios have over-projected CO_2 emissions and economic growth. Environmental Research Letters, 16(1), 014016. https://doi.org/10.1088/1748-9326/abcdd2

Cai, W., McPhaden, M. J., Grimm, A. M., Rodrigues, R. R., Taschetto, A. S., Garreaud, R. D., et al., (2020). Climate impacts of the El Niño–Southern Oscillation on South America.

Nature Reviews Earth & Environment, 1(4), 215–231. https://doi.org/10.1038/s43017-020-0040-3

Castelao, R. M., & Barth, J. A. (2006). Upwelling around Cabo Frio, Brazil: The importance of wind stress curl. Geophysical Research Letters, 33(3), 2005GL025182. https://doi.org/10.1029/2005GL025182

Chakraborty, T., Venter, Z. S., Qian, Y., & Lee, X. (2022). Lower Urban Humidity Moderates Outdoor Heat Stress. AGU Advances, 3(5), e2022AV000729. https://doi.org/10.1029/2022AV000729

Cheng, Y.-T., Lung, S.-C. C., & Hwang, J.-S. (2019). New approach to identifying proper thresholds for a heat warning system using health risk increments. Environmental Research, 170, 282–292. https://doi.org/10.1016/j.envres.2018.12.059

Cirino, P. H., Féres, J. G., Braga, M. J., & Reis, E. (2015). Assessing the Impacts of ENSO-related Weather Effects on the Brazilian Agriculture. Procedia Economics and Finance, 24, 146–155. https://doi.org/10.1016/S2212-5671(15)00635-8

Coelho, C. A. S., De Souza, D. C., Kubota, P. Y., Cavalcanti, I. F. A., Baker, J. C. A., Figueroa, S. N., et al., (2022). Assessing the representation of South American monsoon features in Brazil and U.K. climate model simulations. Climate Resilience and Sustainability, 1(1), e27. https://doi.org/10.1002/cli2.27

Collins, J. M., Chaves, R. R., & Marques, V. da S. (2009). Temperature Variability over South America. Journal of Climate, 22(22), 5854–5869. https://doi.org/10.1175/2009JCLI2551.1

Cordero Simões dos Reis, N., Boiaski, N. T., & Ferraz, S. E. T. (2019). Characterization and Spatial Coverage of Heat Waves in Subtropical Brazil. Atmosphere, 10(5), 284. https://doi.org/10.3390/atmos10050284

Correio Braziliense. (2023, November 18). Rio bate recorde de calor do ano neste sábado (18/11) com 42,5°C. Retrieved May 14, 2024, from https://www.correiobraziliense.com.br/brasil/2023/11/6657444-rio-bate-recorde-de-calor-do-ano-neste-sabado-18-11-com-425-c.html

De Freitas, C., & Grigorieva, E. (2015). Role of Acclimatization in Weather-Related Human Mortality During the Transition Seasons of Autumn and Spring in a Thermally Extreme

Mid-Latitude Continental Climate. International Journal of Environmental Research and Public Health, 12(12), 14974–14987. https://doi.org/10.3390/ijerph121214962

Dereczynski, C., Silva, W. L., & Marengo, J. (2013). Detection and Projections of Climate Change in Rio de Janeiro, Brazil, 2013. https://doi.org/10.4236/ajcc.2013.21003

Diniz, F. R., Gonçalves, F. L. T., & Sheridan, S. (2020). Heat Wave and Elderly Mortality: Historical Analysis and Future Projection for Metropolitan Region of São Paulo, Brazil. Atmosphere, 11(9), 933. https://doi.org/10.3390/atmos11090933

Dunn, R. J. H. (2019). HadISD version 3: monthly updates. Hadley Centre Technical Note.

Espinoza, J.-C., Jimenez, J. C., Marengo, J. A., Schongart, J., Ronchail, J., Lavado-Casimiro, W., & Ribeiro, J. V. M. (2024). The new record of drought and warmth in the Amazon in 2023 related to regional and global climatic features. Scientific Reports, 14(1), 8107. https://doi.org/10.1038/s41598-024-58782-5

Feron, S., Cordero, R. R., Damiani, A., Llanillo, P. J., Jorquera, J., Sepulveda, E., et al., (2019). Observations and Projections of Heat Waves in South America. Scientific Reports, 9(1), 8173. https://doi.org/10.1038/s41598-019-44614-4

Fu, R., Yin, L., Li, W., Arias, P. A., Dickinson, R. E., Huang, L., et al., (2013). Increased dry-season length over southern Amazonia in recent decades and its implication for future climate projection. Proceedings of the National Academy of Sciences, 110(45), 18110–18115. https://doi.org/10.1073/pnas.1302584110

Geirinhas, J. L., Russo, A. C., Libonati, R., Miralles, D. G., Sousa, P. M., Wouters, H., & Trigo, R. M. (2022). The influence of soil dry-out on the record-breaking hot 2013/2014 summer in Southeast Brazil. Scientific Reports, 12(1), 5836. https://doi.org/10.1038/s41598-022-09515-z

Geirinhas, João L., Trigo, R. M., Libonati, R., Coelho, C. A. S., & Palmeira, A. C. (2018). Climatic and synoptic characterization of heat waves in Brazil. International Journal of Climatology, 38(4), 1760–1776. https://doi.org/10.1002/joc.5294

Geirinhas, João L., Trigo, R. M., Libonati, R., Castro, L. C. O., Sousa, P. M., Coelho, C. A. S., et al., (2019). Characterizing the atmospheric conditions during the 2010 heatwave in Rio de Janeiro marked by excessive mortality rates. Science of The Total Environment, 650, 796–808. https://doi.org/10.1016/j.scitotenv.2018.09.060

720   Geirinhas, João L., Russo, A., Libonati, R., Trigo, R. M., Castro, L. C. O., Peres, L. F., et al.,
721   (2020). Heat-related mortality at the beginning of the twenty-first century in Rio de
722   Janeiro, Brazil. International Journal of Biometeorology, 64(8), 1319–1332.
723   https://doi.org/10.1007/s00484-020-01908-x
724   Geirinhas, João L., Russo, A., Libonati, R., Sousa, P. M., Miralles, D. G., & Trigo, R. M. (2021).
725   Recent increasing frequency of compound summer drought and heatwaves in Southeast
726   Brazil. Environmental Research Letters, 16(3), 034036. https://doi.org/10.1088/1748-
727   9326/abe0eb
728   Gomes, G.D., Nunes, A.M.B., Libonati, R., & Ambrizzi, T. (2022). Projections of subcontinental
729   changes in seasonal precipitation over the two major river basins in South America under
730   an extreme climate scenario. Climate Dynamics, 58, 1147–1169.
731   https://doi.org/10.1007/s00382-021-05955-x
732   Grimm, A. M. (2019). Madden–Julian Oscillation impacts on South American summer monsoon
733   season: precipitation anomalies, extreme events, teleconnections, and role in the MJO
734   cycle. Climate Dynamics, 53(1), 907–932. https://doi.org/10.1007/s00382-019-04622-6
735   Hausfather, Z., & Peters, G. P. (2020). Emissions – the 'business as usual' story is misleading.
736   Nature, 577(7792), 618–620. https://doi.org/10.1038/d41586-020-00177-3
737   He, Z., Dai, A., & Vuille, M. (2021). The Joint Impacts of Atlantic and Pacific Multidecadal
738   Variability on South American Precipitation and Temperature. Journal of Climate,
739   34(19), 7959–7981. https://doi.org/10.1175/JCLI-D-21-0081.1
740   Hersbach, H., Bell, B., Berrisford, P., Hirahara, S., Horányi, A., Muñoz-Sabater, J., et al., (2020).
741   The ERA5 global reanalysis. Quarterly Journal of the Royal Meteorological Society,
742   146(730), 1999–2049. https://doi.org/10.1002/qj.3803
743   Horowitz, M. (2016). Epigenetics and cytoprotection with heat acclimation. Journal of Applied
744   Physiology (Bethesda, Md.: 1985), 120(6), 702–710.
745   https://doi.org/10.1152/japplphysiol.00552.2015
746   Huang, B., Liu, C., Banzon, V., Freeman, E., Graham, G., Hankins, B., et al., (2021).
747   Improvements of the Daily Optimum Interpolation Sea Surface Temperature (DOISST)
748   Version 2.1. Journal of Climate, 34(8), 2923–2939. https://doi.org/10.1175/JCLI-D-20-
749   0166.1

Hughs, E., & Jeantet, D. (2023, November 15). It's not yet summer in Brazil, but a dangerous heat wave is sweeping the country. Retrieved May 14, 2024, from https://apnews.com/article/brazil-heat-wave-climate-environment-wildfires-1e4714fb2c6566120c13cf4e2b657f7d

Instituto Brasileiro de Geografia e Estatística. (2022). Demographic Census 2022. Retrieved from https://sidra.ibge.gov.br/pesquisa/censo-demografico/demografico-2022/primeiros-resultados-populacao-e-domicilios

Ivanovich, C. C., Horton, R. M., Sobel, A. H., & Singh, D. (2024). Subseasonal Variability of Humid Heat During the South Asian Summer Monsoon. Geophysical Research Letters, 51(6), e2023GL107382. https://doi.org/10.1029/2023GL107382

Jones, C., & Carvalho, L. M. V. (2013). Climate change in the South American Monsoon System: Present climate and CMIP5 projections. Journal of Climate, 26(17), 6660–6678. https://doi.org/10.1175/JCLI-D-12-00412.1

Jornal Nacional. (2023, November 18). Taylor Swift: segundo show é adiado, por causa do calor extremo no Rio. Retrieved April 16, 2024, from https://g1.globo.com/jornal-nacional/noticia/2023/11/18/taylor-swift-show-e-adiado-apos-morte-de-fa.ghtml

Krüger, E., Gobo, J. P. A., Tejas, G. T., da Silva de Souza, R. M., Neto, J. B. F., Pereira, G., et al., (2024). The impact of urbanization on heat stress in Brazil: A multi-city study. Urban Climate, 53, 101827. https://doi.org/10.1016/j.uclim.2024.101827

Lanzante, J. R., Dixon, K. W., Nath, M. J., Whitlock, C. E., & Adams-Smith, D. (2018). Some Pitfalls in Statistical Downscaling of Future Climate. Bulletin of the American Meteorological Society, 99(4), 791–803. https://doi.org/10.1175/BAMS-D-17-0046.1

Latinović, D., Chou, S. C., Rančić, M., Medeiros, G. S., & Lyra, A. D. A. (2019). Seasonal climate and the onset of the rainy season in western-central Brazil simulated by Global Eta Framework model. International Journal of Climatology, 39(3), 1429–1445. https://doi.org/10.1002/joc.5892

Lemus-Canovas, M., Insua-Costa, D., Trigo, R. M., & Miralles, D. G. (2024). Record-shattering 2023 Spring heatwave in western Mediterranean amplified by long-term drought. Npj Climate and Atmospheric Science, 7(1), 1–8. https://doi.org/10.1038/s41612-024-00569-6

780   Libonati, R., Geirinhas, J. L., Silva, P. S., Monteiro Dos Santos, D., Rodrigues, J. A., Russo, A.,

781   et al., (2022). Drought–heatwave nexus in Brazil and related impacts on health and fires:

782   A comprehensive review. Annals of the New York Academy of Sciences, 1517(1), 44–

783   62. https://doi.org/10.1111/nyas.14887

784   Liebmann, B., & Mechoso, C. R. (2011). THE SOUTH AMERICAN MONSOON SYSTEM. In

785   C.-P. Chang, Y. Ding, N.-C. Lau, R. H. Johnson, B. Wang, & T. Yasunari, World

786   Scientific Series on Asia-Pacific Weather and Climate (2nd ed., Vol. 5, pp. 137–157).

787   WORLD SCIENTIFIC. https://doi.org/10.1142/9789814343411_0009

788   Lyra, G. B., Correia, T. P., de Oliveira-Júnior, J. F., & Zeri, M. (2018). Evaluation of methods of

789   spatial interpolation for monthly rainfall data over the state of Rio de Janeiro, Brazil.

790   Theoretical and Applied Climatology, 134(3), 955–965. https://doi.org/10.1007/s00704-

791   017-2322-3

792   Marengo, J. A., Liebmann, B., Grimm, A. M., Misra, V., Silva Dias, P. L., Cavalcanti, I. F. A., et

793   al., (2012). Recent developments on the South American monsoon system. International

794   Journal of Climatology, 32(1), 1–21. https://doi.org/10.1002/joc.2254

795   Marengo, Jose A., Soares, W. R., Saulo, C., & Nicolini, M. (2004). Climatology of the Low-

796   Level Jet East of the Andes as Derived from the NCEP–NCAR Reanalyses:

797   Characteristics and Temporal Variability. Journal of Climate, 17(12), 2261–2280.

798   https://doi.org/10.1175/1520-0442(2004)017<2261:COTLJE>2.0.CO;2

799   Montini, T. L., Jones, C., & Carvalho, L. M. V. (2019). The South American Low-Level Jet: A

800   New Climatology, Variability, and Changes. Journal of Geophysical Research:

801   Atmospheres, 124(3), 1200–1218. https://doi.org/10.1029/2018JD029634

802   Mora, C., Dousset, B., Caldwell, I. R., Powell, F. E., Geronimo, R. C., Bielecki, C. R., et

803   al., (2017). Global risk of deadly heat. Nature Climate Change, 7(7), 501–506.

804   https://doi.org/10.1038/nclimate3322

805   Nahlik, M. J., Chester, M. V., Pincetl, S. S., Eisenman, D., Sivaraman, D., & English, P. (2017).

806   Building Thermal Performance, Extreme Heat, and Climate Change. Journal of

807   Infrastructure Systems, 23(3), 04016043. https://doi.org/10.1061/(asce)is.1943-

808   555x.0000349

809 NASA JPL. (2024, January 23). El Niño 2023 | El Niño/La Niña Watch & PDO. Retrieved May
810   14, 2024, from https://sealevel.jpl.nasa.gov/data/el-nino-la-nina-watch-and-pdo/el-nino-
811   2023
812 Nguyen, B. (2023, December 27). Brazilian Taylor Swift Fan Died Of Heat Exhaustion At Rio
813   Concert. Retrieved April 16, 2024, from
814   https://www.forbes.com/sites/britneynguyen/2023/12/27/brazilian-taylor-swift-fan-died-
815   of-heat-exhaustion-at-rio-concert/
816 Palma, E. D., & Matano, R. P. (2009). Disentangling the upwelling mechanisms of the South
817   Brazil Bight. Continental Shelf Research, 29(11), 1525–1534.
818   https://doi.org/10.1016/j.csr.2009.04.002
819 Pascale, S., Carvalho, L. M. V., Adams, D. K., Castro, C. L., & Cavalcanti, I. F. A. (2019).
820   Current and Future Variations of the Monsoons of the Americas in a Warming Climate.
821   Current Climate Change Reports, 5(3), 125–144. https://doi.org/10.1007/s40641-019-
822   00135-w
823 Pepin, N., Bradley, R. S., Diaz, H. F., Baraer, M., Caceres, E. B., Forsythe, N., et al., (2015).
824   Elevation-dependent warming in mountain regions of the world. Nature Climate Change,
825   5(5), 424–430. https://doi.org/10.1038/nclimate2563
826 Périard, J. D., Racinais, S., & Sawka, M. N. (2015). Adaptations and mechanisms of human heat
827   acclimation: Applications for competitive athletes and sports. Scandinavian Journal of
828   Medicine & Science in Sports, 25 Suppl 1, 20–38. https://doi.org/10.1111/sms.12408
829 Powis, C. M., Byrne, D., Zobel, Z., Gassert, K. N., Lute, A. C., & Schwalm, C. R. (2023).
830   Observational and model evidence together support wide-spread exposure to
831   noncompensable heat under continued global warming. Science Advances, 9(36),
832   eadg9297. https://doi.org/10.1126/sciadv.adg9297
833 Perkins, S. E., Pitman, A. J., Holbrook, N. J., & McAneney, J. (2007). Evaluation of the AR4
834   Climate Models' Simulated Daily Maximum Temperature, Minimum Temperature, and
835   Precipitation over Australia Using Probability Density Functions. Journal of Climate,
836   20(17), 4356–4376. https://doi.org/10.1175/JCLI4253.1
837 Raia, A., & Cavalcanti, I. F. A. (2008). The Life Cycle of the South American Monsoon System.
838   Journal of Climate, 21(23), 6227–6246. https://doi.org/10.1175/2008JCLI2249.1

839   Raymond, C., & Mankin, J. S. (2019). Assessing present and future coastal moderation of
840   extreme heat in the Eastern United States. Environmental Research Letters, 14(11),
841   114002. https://doi.org/10.1088/1748-9326/ab495d
842   Raymond, C., Matthews, T., & Horton, R. M. (2020). The emergence of heat and humidity too
843   severe for human tolerance. Science Advances, 6(19), eaaw1838.
844   https://doi.org/10.1126/sciadv.aaw1838
845   Raymond, C., Waliser, D., Guan, B., Lee, H., Loikith, P., Massoud, E., et al., (2022). Regional
846   and Elevational Patterns of Extreme Heat Stress Change in the US. Environmental
847   Research Letters. https://doi.org/10.1088/1748-9326/ac7343
848   Regoto, P., Dereczynski, C., Chou, S. C., & Bazzanela, A. C. (2021). Observed changes in air
849   temperature and precipitation extremes over Brazil. International Journal of Climatology,
850   41(11), 5125–5142. https://doi.org/10.1002/joc.7119
851   Rehbein, A., & Ambrizzi, T. (2023). ENSO teleconnections pathways in South America. Climate
852   Dynamics, 61(3), 1277–1292. https://doi.org/10.1007/s00382-022-06624-3
853   Ritchie, J., & Dowlatabadi, H. (2017). Why do climate change scenarios return to coal? Energy,
854   140, 1276–1291. https://doi.org/10.1016/j.energy.2017.08.083
855   Rogero, T. (2024, May 19). Brazil counts cost of worst-ever floods with little hope of waters
856   receding soon. The Guardian. Retrieved from
857   https://www.theguardian.com/world/article/2024/may/19/brazil-floods-toll
858   Rogers, C. D. W., Ting, M., Li, C., Kornhuber, K., Coffel, E. D., Horton, R. M., et al., (2021).
859   Recent Increases in Exposure to Extreme Humid-Heat Events Disproportionately Affect
860   Populated Regions. Geophysical Research Letters, 48(19).
861   https://doi.org/10.1029/2021GL094183
862   Shimizu, M. H., & Ambrizzi, T. (2016). MJO influence on ENSO effects in precipitation and
863   temperature over South America. Theoretical and Applied Climatology, 124(1), 291–301.
864   https://doi.org/10.1007/s00704-015-1421-2
865   Shreevastava, A., Raymond, C., & Hulley, G. C. (2023). Contrasting Intraurban Signatures of
866   Humid and Dry Heatwaves over Southern California. Journal of Applied Meteorology
867   and Climatology, 62(6), 709–720. https://doi.org/10.1175/JAMC-D-22-0149.1
868   Sistema Alerta Rio da Prefeitura do Rio de Janeiro. (2024). Meteorological Data. Retrieved from
869   https://alertario.rio.rj.gov.br/download/dados-meteorologicos/

870   Sistema IBGE de Recuperação Automática - SIDRA. (n.d.). Retrieved April 21, 2024, from

871   https://sidra.ibge.gov.br/pesquisa/censo-demografico/demografico-2022/primeiros-

872   resultados-populacao-e-domicilios

873   Son, J.-Y., Gouveia, N., Bravo, M. A., de Freitas, C. U., & Bell, M. L. (2016). The impact of

874   temperature on mortality in a subtropical city: effects of cold, heat, and heat waves in São

875   Paulo, Brazil. International Journal of Biometeorology, 60(1), 113–121.

876   https://doi.org/10.1007/s00484-015-1009-7

877   Stefanello, M., Ewerling da Rosa, C., Bresciani, C., Cordero Simões dos Reis, N., Stefanello

878   Facco, D., Teleginski Ferraz, S. E., et al., (2022). Spatial–temporal analysis of a summer

879   heat wave associated with downslope flows in southern Brazil: implications in the

880   atmospheric boundary layer. Atmosphere 14(1). 64.

881   https://doi.org/10.3390/atmos14010064

882   Swann, A. L. S., Longo, M., Knox, R. G., Lee, E., & Moorcroft, P. R. (2015). Future

883   deforestation in the Amazon and consequences for South American climate. Agricultural

884   and Forest Meteorology, 214–215, 12–24.

885   https://doi.org/10.1016/j.agrformet.2015.07.006

886   Tan, J., Zheng, Y., Tang, X., Guo, C., Li, L., Song, G., et al., (2010). The urban heat island and

887   its impact on heat waves and human health in Shanghai. International Journal of

888   Biometeorology, 54(1), 75–84. https://doi.org/10.1007/s00484-009-0256-x

889   Thrasher, B., Wang, W., Michaelis, A., Melton, F., Lee, T., & Nemani, R. (2022). NASA Global

890   Daily Downscaled Projections, CMIP6. Scientific Data, 9(1), 262.

891   https://doi.org/10.1038/s41597-022-01393-4

892   United Nations Department of Economic and Social Affairs Population Division. (2022).

893   Population of Urban Agglomerations with 300,000 Inhabitants or More in 2018, by

894   country, 1950-2035 (thousands). Retrieved from

895   https://population.un.org/wup/Download/

896   US EPA, O. (2021, February 4). Climate Change Indicators: Heat Waves [Reports and

897   Assessments]. Retrieved April 23, 2024, from https://www.epa.gov/climate-

898   indicators/climate-change-indicators-heat-waves

899   Vecellio, D. J., Wolf, S. T., Cottle, R. M., & Kenney, W. L. (2022). Evaluating the 35°C wet-

900   bulb temperature adaptability threshold for young, healthy subjects (PSU HEAT Project).

901   Journal of Applied Physiology, 132(2), 340–345.

902   https://doi.org/10.1152/japplphysiol.00738.2021

903 Vera, C., Baez, J., Douglas, M., Emmanuel, C. B., Marengo, J., Meitin, J., et al., (2006). The

904   South American Low-Level Jet Experiment. Bulletin of the American Meteorological

905   Society, 87(1), 63–78. https://doi.org/10.1175/BAMS-87-1-63

906 Wilby, R. L., Kasei, R., Gough, K. V., Amankwaa, E. F., Abarike, M., Anderson, N. J., et al.,

907   (2021). Monitoring and moderating extreme indoor temperatures in low-income urban

908   communities. Environmental Research Letters, 16(2), 024033.

909   https://doi.org/10.1088/1748-9326/abdbf2

910 You, Y., Ting, M., & Biasutti, M. (2024). Climate warming contributes to the record-shattering

911   2022 Pakistan rainfall. Npj Climate and Atmospheric Science, 7(1), 1–8.

912   https://doi.org/10.1038/s41612-024-00630-4

913 Zhao, Q., Li, S., Coelho, M. S. Z. S., Saldiva, P. H. N., Hu, K., Huxley, R. R., et al., (2019). The

914   association between heatwaves and risk of hospitalization in Brazil: A nationwide time

915   series study between 2000 and 2015. PLOS Medicine, 16(2), e1002753.

916   https://doi.org/10.1371/journal.pmed.1002753